

# Endophytic Bacteria (*Bacillus albus*) Mediated Silver Nanoparticles Induce Cytotoxicity in Triple Negative Breast Cancer Cells

Shariq Ahamed Mustaq<sup>1</sup>, Mohamed Juvad Najeer Ahamed<sup>1</sup>, Hemalatha Srinivasan<sup>1,\*</sup> 

<sup>1</sup> School of Life Sciences, B. S. Abdur Rahman Crescent Institute of Science and Technology, Vandalur, Chennai– 600048, India; shariqahmedm27@gmail.com (S.A.M.); juvads17@gmail.com (M.J.N.A.); hemalatha.sls@crecident.education (H.S.);

\* Correspondence:hemalatha.sls@crecident.education;

Received: 23.08.2023; Accepted: 12.05.2024; Published: 25.11.2025

**Abstract:** Endophytes are a group of microorganisms that reside inside the tissues of the plant. In this study, endophytic bacteria were isolated from marine seaweed (*Chaetomorpha antennina*), which is capable of producing novel bioactive compounds. Isolation and identification of the endophytic bacteria by 16S rRNA sequencing. *In silico* analysis (Lipinski's screening, Swiss ADME, Virtual screening of compounds, and molecular docking) was performed for the phytochemicals present in endophytic bacteria. Silver nanoparticles (AgNPs) were biosynthesized using the endophytic bacteria and characterized by UV-visible, FTIR spectroscopy, FESEM, EDX, and DLS for various physicochemical and morphological properties and to screen the anticancer activity of AgNPs in MDM-MB231 breast cancer cell lines by MTT assay. The isolated endophytic bacteria were identified as *Bacillus albus*. The phytochemicals of *B. albus* were able to bind with the Bcl-2 is 2-(6-{1-ethyl-4-[4-(1H-pyrrol-2-ylcarbonyl)-2,3,3a,4,5,7a-hexahydro-1H-inden-5-yl]-1,3-butadienyl}-5-methyltetrahydro-2H-pyran-2-yl) propanoate, and binding energy was found as -8.38 kcal/mol, and Calcifediol with Bax is -8.28kcal/mol. The AgNPs showed effective anticancer activity against MDM-MB-231 breast cancer cells at varying concentrations, with cell viability being concentration-dependent. The phytochemicals were able to bind with anti-apoptotic protein and pro-apoptotic proteins and induced cytotoxicity in MDM-MB-231, and phytochemicals incorporated AgNPs were able to induce cytotoxicity, and these novel endophytic nanoparticles can be incorporated in cancer drug formulations; however, further *in vivo* studies are warranted.

**Keywords:** endophytes; silver nanoparticles; breast cancer; MDM-MB-231.

© 2025 by the authors. This article is an open-access article distributed under the terms and conditions of the Creative Commons Attribution (CC BY) license (<https://creativecommons.org/licenses/by/4.0/>), which permits unrestricted use, distribution, and reproduction in any medium, provided the original work is properly cited. The authors retain copyright of their work, and no permission is required from the authors or the publisher to reuse or distribute this article, as long as proper attribution is given to the original source.

## 1. Introduction

Breast cancer is the second most widespread cancer after lung cancer. It is a type of cancer or malignant tumor that occurs in the breast tissues of women [1]. Breast cancer is synonymous with women; even men have been diagnosed with breast cancer, referred to as male breast cancer (MBC). One percent of the total breast cancer cases occurred in men [2,3]. Even though the exact cause of breast cancer is unknown, factors including genetics, family history, age, and lifestyle habits such as smoking or consuming alcohol play a major role [3].

The symptoms may vary from person to person, but the major symptoms include physical changes in the affected tissue, lumps, and changes in skin color leading to redness [4].

Breast cancer can be easily cured if diagnosed at an early stage, and the treatments include chemotherapy, immunotherapy, radiation therapy, hormonal therapy, and targeted therapy [5]. In recent years, novel treatment methods have been in demand due to chemoresistance or resistance against anticancer drugs [6]. Nanotechnological approaches have emerged as promising strategies for breast cancer treatment using nanoparticles, nanocarriers, dendrimers, quantum dots, etc., with greater efficacy against breast cancer and reduced toxicity to healthy tissues through targeted therapy [7].

Bionanotechnology emerged by combining biology and technology to develop nanoparticles/nanomaterials and find solutions for deadly diseases. There are two approaches to the synthesis of nanoparticles: top-down (Mechanical milling, Laser ablation, sputtering, chemical etching) and bottom-up (sol-gel, aerosol process, biological methods using bacteria, fungi, plant extracts, etc.). Although there are several types of metal nanoparticles, including gold, copper, zinc, iron oxide, etc., silver nanoparticles have received significant attention from researchers due to their unique characteristics and wide spectrum of applications in the fields of medicine, pharmaceuticals, agriculture, food science, and other interdisciplinary areas [8,9]. Eco-friendly methods for nanoparticle synthesis using microorganisms, plants, and algae are natural, eco-friendly, biocompatible, scalable, and cost-effective; thus, they have been in high demand for the past several decades [10]. Instead of using toxic chemicals in chemically mediated synthesis, which is non-cost-efficient, energy-intensive, and time-consuming, it uses high-energy methods.

Endophytes are beneficial microorganisms, such as bacteria, fungi, and actinomycetes, that reside within the internal tissues of plants, including roots, shoots, leaves, and flowers. Endophytes are beneficial microbes that play an important role in plant development, help as a defense mechanism, protect the plants from invading pathogens and insects, and promote plant growth [11,12]. The endophytic bacteria used for the current study were isolated from marine seaweed. Marine seaweeds are a group of plants/algae that grow on the ocean's coastal surfaces and are attached to the rocks. It is reported that endophytic microorganisms produce novel bioactive metabolites because they are exposed to various biotic and abiotic stresses, such as sunlight, salinity, pH, temperature, desiccation during low tides, UV radiation, and pathogens. The bioactive compounds secreted by the microorganisms are industrially important enzymes and pharmaceutical drugs that play an important role in biological applications [13-15].

In this research paper, the endophytic bacteria were isolated from the seaweed and identified as *Bacillus albus*. The bacterial crude extract was prepared and analyzed for the phytocompounds present in the extract by GC-MS, *In silico* analysis was performed to screen for the binding efficiency of the phytocompounds with apoptotic proteins (Bcl-2 and BAX). Further, the crude extract was used for the biogenic synthesis of silver nanoparticles, which were characterized by UV-Visible spectroscopy, FT-IR, DLS, and FESEM-EDAX. The cytotoxic effect of synthesized silver nanoparticles was evaluated in Triple-negative breast cancer lines (MDA-MB-231).

## 2. Materials and Methods

### 2.1. Isolation and identification of endophytic bacteria.

The endophytic bacteria were isolated from a marine seaweed freshly collected from Kovalam, Chennai, India (12.7870°N, 80.2504°E), washed three times with tap water, then twice with distilled water, before surface sterilization. The surface sterilization of the seaweed was performed in sequence: 70% ethanol, 1% Sodium hypochlorite solution, 70% ethanol, and finally distilled water (each immersion lasting 1-2 minutes). Then, the seaweed filaments were blot-dried aseptically and placed on Luria-Bertani Agar (LBA) plates under aseptic conditions. The plates were incubated at 37°C and monitored for up to 3 days until bacterial colonies were observed growing around the filaments. Then, the inoculum was streaked onto another plate to obtain pure colonies, incubated at 37°C for 24h, and the culture was maintained continuously. Gram staining was performed to determine the bacteria's morphology. The bacterial identification was performed by DNA isolation, amplification with 16S primers, and sequencing. BLAST analyzed the sequencing results to identify the bacterial species using MEGA-X software [16].

### 2.2. Preparation of bacterial crude extract for GC-MS analysis.

The 24h-incubated bacterial culture was centrifuged; the pellet was washed and then sonicated, and the supernatant was collected after centrifugation (10000 RPM/10 minutes) and freeze-dried in a freeze-dryer. The obtained sample was subjected to solid-liquid extraction with methanol and then left to open-air evaporation. Then, the crude bacterial extract was obtained by adding methanol, filtering the solution through a 0.45 µM pore syringe filter, and using it for GC-MS analysis [17].

### 2.3. *In silico* analysis.

#### 2.3.1. Preparation and Swiss ADME analysis of phytochemicals from endophytic bacteria.

The 3-D structures of phytochemicals were retrieved from the PubChem database in PDF format. The phytochemicals were screened for drug-like properties using Lipinski's rule of five [18]. In order to understand the pharmacokinetically active molecules, ADME analysis was performed using the Swiss ADME server [19].

#### 2.3.2. Preparation of proteins.

The 3-D structures of apoptotic proteins, such as BAX (PDB ID: 1F16) and BCL-2 (PDB ID:1G5M), were downloaded from the Protein Data Bank.

#### 2.3.3. Virtual screening and molecular docking.

The protein structure was prepared in BIOVIA Discovery Studio by removing water molecules and heteroatoms, adding polar hydrogens, and computing charges. The target proteins were loaded into the PyRx application using the AutoDock plugin. The PDB format of the target proteins was converted to PDBQT. The ligand energies were minimized and converted to PDBQT format after the phytochemicals were uploaded. The target proteins and phytochemicals of the extract are selected using the Vina wizard option, and the gridbox view is refined and modified, followed by blind virtual screening [20]. After the virtual screening of

ligands, phytochemicals with binding affinity greater than  $-5.5$  kcal/mol were subjected to molecular docking using AutoDock 4.2.6. Later, the interactions of the compounds with the target proteins were analyzed using the Discovery Studio visualizer.

#### 2.4. Biosynthesis and characterization of endophytic silver nanoparticles.

The biosynthesis of silver nanoparticles (AgNPs) using the endophytic bacteria was carried out by growing the bacterial culture in LB broth at  $37^{\circ}\text{C}$  for 2 days under agitation. The obtained bacterial cells were centrifuged at 10,000 rpm for 10 minutes, and the supernatant was collected. The biosynthesis of AgNPs was optimized using different ratios of bacterial supernatant and 1 mM Silver nitrate ( $\text{AgNO}_3$ ) solution, ranging from 1:1 to 1:5, with the supernatant constant and the silver nitrate ratio varying. The mixture was left at room temperature for up to 2h and was observed for color change. The AgNPs were characterized by UV-visible and FT-IR spectroscopy, FESEM, EDX, DLS, and XRD for physicochemical characterization of the synthesized AgNPs [21].

#### 2.5. Anticancer assay by using AgNPs.

The anticancer effect of synthesized AgNPs was evaluated using an MTT assay. MDA-MB-231, which was used to assess the cytotoxicity of the AgNPs, is a breast cancer cell line. Around 80-85% of the confluent cells were seeded in the 96-well plate, and once the cells were grown, they were treated with AgNPs (Control, 2.5, 5, 10, 20  $\mu\text{g/ml}$ ) and incubated for 24 hours. 100  $\mu\text{l}$  of MTT (0.5 mg/mL) was added and incubated in a  $\text{CO}_2$  incubator for 2 hours. After removing the dyes, 100  $\mu\text{l}$  of DMSO was added to the plate, mixed, and kept in the dark for 15 minutes; the OD was measured at A570 [20].

### 3. Results and Discussion

#### 3.1. Isolation and identification of endophytic bacteria.

The endophytic bacteria isolated from the marine seaweed were found to be rod-shaped and Gram-positive. The molecular characterization revealed that the isolated bacteria were *Bacillus albus*, as determined by BLAST analysis (Figure 1C). The bacteria are Gram-positive and rod-shaped Figure 1A. The GC-MS spectrum of the *Bacillus albus* extract is shown in Figure 1B, and these compounds were used to screen for binding affinities with apoptotic proteins (Bax and Bcl2). Endophytic bacteria are endophytes that produce secondary metabolites by residing inside the host. The endophytic bacteria isolated from seaweed were identified as *Bacillus albus*. *Bacillus* sp. is known to produce various phytochemicals and has biological activities, including antibacterial, antifungal, and anticancer activities [22]. The GC-MS analysis of the bacterial crude extract identified the phytochemicals and was used to assess binding efficiency with Bcl-2 and Bax. Lipinski's rule of five was performed to screen the drug-like properties of the molecules. For a molecule to be successful, it must follow any of these two rules: i) molecular mass should be less than 500 kDa, ii) hydrogen donor should be less than 5, iii) hydrogen acceptor should be less than 10, iv) lipophilicity should be less than 5 and v) molar refractivity should be in the range between 40- 130 [18]. All the phytochemicals from the bacterial crude extract did not violate Lipinski's screening, and all the phytochemicals possess drug-like properties, unlike the standard drug doxorubicin.

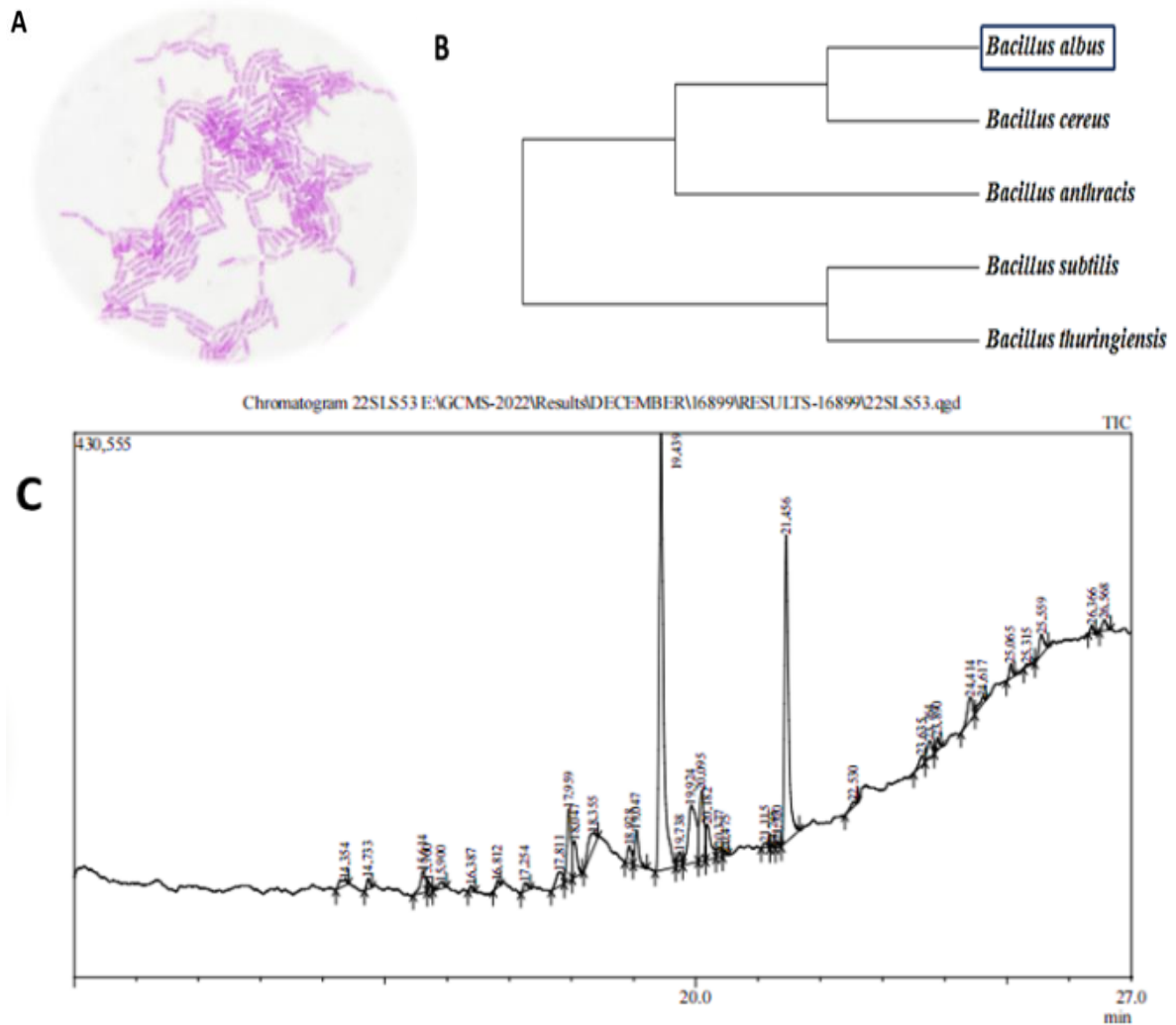


**Figure 1.** (A) Gram staining of *Bacillus albus*; (B) Phylogenetic relationship of endophytic bacteria *Bacillus albus* isolated from seaweed with other isolates using MEGA-X, Maximum likelihood method with other related strains retrieved from NCBI GenBank; (C) GC-MS spectrum of crude extract of *Bacillus albus*.

### 3.2. *In silico* analysis.

Lipinski's screening of phytochemicals from *B. albus* was analyzed and represented in Table 1. All the compounds present in the extract of *B. albus* did not violate the drug-likeness properties of a molecule, except the standard drug doxorubicin used for the study. SwissADME analysis was performed for the phytochemicals of *B. albus* (Table 2). The ESOL water solubility, GI- absorption, BBB permeability (Blood-brain barrier), CYP3A4 inhibitor, and bioavailability were analyzed. The oral bioavailability, water solubility, and GI absorption were lower in the standard drug doxorubicin. It is also a P-gp substrate, which can be easily effluxed from cancerous cells.

**Table 1.** Lipinski screening of phytochemicals from *B. albus*.

S. No	PubChem ID	Compounds	Molecular weight	Hydrogen donor	Hydrogen acceptors	LogP lipophilicity	Molar refractivity	No of violations
1	91694673	Benzene sulfonamide,3-amino-N-methyl-N-octadecyl-	438	2	4	8.231602	130.2604	1
2	17081	Decanedioic acid, didecylester	482	0	4	9.475004	144.0741	1
3	17152	1,1'-oxybisdecane	298	0	1	7.284402	96.03896	1
4	87077689	Dodecylnonyl ether	312	0	1	7.674502	100.656	1
5	22434	Heneicosanoic acid, methylester	340	0	2	7.591202	105.413	1
6	41517	Heptacosanoic acid, methylester	424	0	2	9.931806	133.115	1
7	12400	Triacontanoic acid, methylester	466	0	2	11.10211	146.9661	1
8	8201	Octadecanoic acid, methylester	298	0	2	6.420901	91.56197	1
9	6439696	9-octadecenoic acid (z)-	312	5	6	-0.0531	77.14578	0
10	5281	Octadecanoic acid	284	1	2	6.3325	87.18177	1
11	167795	Tetradecanoic acid,12-methyl-, methyl ester,(S)-	316	2	4	3.829899	89.67656	0
12	5354176	9-octadecenoic acid,12-(acetyloxy)-, methylester,[r-(z)]-	354	0	4	5.7385	102.405	0
13	14259	Eicosanoic acid, methylester	326	0	2	7.201102	100.796	1
14	15609	Heptadecanoic acid, methylester	284	0	2	6.0308	86.94497	1
15	14026379	Methyl octadecylether	284	0	1	6.894301	91.42196	1
16	12620	1-docosanol	326	1	1	7.800603	105.0997	1
17	11001473	Oxiraneoctanoic acid, 3-octyl-,methylester, cis-	312	0	3	5.4081	90.98897	0
18	6440717	Demycarosylturimycin h	312	5	6	-0.0531	77.14578	0
19	753	Glycerin	92	3	3	-1.6681	20.1784	1
20	603751	4-[(2-Hydroxy-phenylimino)-methyl]-5-methyl-2-phenyl-2,4-dihydro-pyrazole-3-one	293	1	5	3.133399	86.78577	0
21	570815	1-bromo-2,2,3,3-tetramethyl-1-(1-propynyl)cyclopropane	214	0	0	3.209399	52.66999	0
22	135580697	2,6-Dihydroxybenzaldehyde, carbamoylhydrazine	195	5	6	0.1	50.0847	0
23	5283731	Calcifediol	400	2	2	6.733902	122.6486	1
24	91897038	2-(6-{1-ethyl-4-[4-(1H-pyrrol-2-ylcarbonyl)-2,3,3a,4,5,7a-hexahydro-1H-inden-5-yl]-1,3-butadienyl}-5-methyltetrahydro-2H-pyran-2-yl)propanoate	464	1	4	4.8782	130.8182	0
25	539493	4-chloro-3,5-dimethylisoxazole#	131	0	2	1.94484	30.987	1
26	66174	2-Amino-5-chloropyridine	128	2	2	1.3172	33.6594	1
27	581866	2-Pyridinamine,4-chloro-	128	2	2	1.3172	33.6594	1
28	23351	Tripropargylamine	131	0	1	0.188	42.939	0
29	68161	Pyridine,2,3,4,5-tetrahydro-	83	0	1	1.2411	27.20999	1
30	10798	1H-Imidazole, 4,5-dihydro-2-methyl-	84	1	2	0	25.9787	1
31	138264	2,3-diethyloxirane	100	0	1	1.5738	29.24299	0

S. No	PubChem ID	Compounds	Molecular weight	Hydrogen donor	Hydrogen acceptors	LogP lipophilicity	Molar refractivity	No of violations
32	1146	Methylamine,N,N-dimethyl-	59	0	1	0.1778	19.611	1
33	96291	1-Hexanol, 5-methyl-2-(1-methylethyl)-	158	1	1	2.6871	49.48578	0
34	70825	Phenol, 3,5-bis(1,1-dimethylethyl)-	206	1	1	3.987199	65.50678	0
35	31405	Phenol, 2,6-bis(1,1-dimethylethyl)-	206	1	1	3.987199	65.50678	0
36	554135	Cyclopentanetridecanoic acid, methylester	296	0	2	6.0308	89.37797	1
37	523245	Methyl6-methyloctanoate	172	0	2	2.7659	49.93898	0
38	31284	Methyl tetradecanoate	242	0	2	4.860499	73.09398	0
39	522345	Hexadecanoic acid,15-methyl-, methylester	284	0	2	5.886701	86.87497	1
40	2969	Decanoicacid	172	1	2	3.211699	50.24579	0
41	13849	Pentadecanoic acid	242	1	2	5.162199	73.33078	0
42	23518	Pentadecanoic acid, methylester	256	0	2	5.2506	77.71098	0
43	521323	Dodecanoic acid,10-methyl-, methylester	228	0	2	4.326299	68.40698	0
44	21204	Tridecanoicacid,12-methyl-, methylester	242	0	2	4.716399	73.02398	0
45	193540	Pyrrolo[1,2-a]pyrazine-1,4-dione, hexahydro-	154	1	4	-0.8928	37.74469	0
46	3013625	Glycyl-L-proline	172	3	5	-0.9793	41.42519	0
47	91704718	1,4-diaza-2,5-dioxobicyclo[4.3.0]nonane	196	0	5	-0.6339	47.12899	0
48	10887	9-Heptadecanone	254	0	1	6.056701	80.99297	0
49	8181	Hexadecanoic acid,methylester	270	0	2	5.6407	82.32797	0
50	21205	Methyl14-methyl pentadecanoate	270	0	2	5.4966	82.25797	0
51	62603	Benzenepropanoicacid,3,5-bis(1,1-dimethylethyl)-4-hydroxy-, methylester	292	1	3	4.092798	85.84377	0
52	545786	4-(3,5-di-tertbutyl4-hydroxyphenyl)butylacrylate	332	1	3	5.0391	99.60076	0
53	985	N-Hexadecanoic acid	256	1	2	5.552299	77.94778	0
54	520159	Hexadecanoicacid,14-methyl-, methylester	284	0	2	5.886701	86.87497	0
55	14957558	Methyl 8,10-octadecadiynoate	290	0	2	4.8673	88.64598	0
56	14957560	Methyl 5,7-hexadecadiynoate	262	0	2	4.087099	79.41198	0
57	14309412	Methyl 7,9-octadecadiynoate	290	0	2	4.8673	88.64598	0
58	14957561	Methyl 9,11-octadecadiynoate	290	0	2	4.8673	88.64598	0
59	14957559	Methyl 10,12-octadecadiynoate	290	0	2	4.8673	88.64598	0
60	8139	Dodecanoicacid,methylester	214	0	2	4.080298	63.85998	0
61	15608	Tridecanoicacid,methylester	228	0	2	4.470399	68.47698	0
62	554144	Undecanoic acid,10-methyl-, methylester	214	0	2	3.936199	63.78998	0
63	8209	1-tetradecanol	214	1	1	4.679799	68.16377	0
64	2682	1-hexadecanol	242	1	1	5.46	77.39777	0
65	5364431	Methyl(7e)-7 hexadecenoate#	268	0	2	5.4167	82.23397	0

S. No	PubChem ID	Compounds	Molecular weight	Hydrogen donor	Hydrogen acceptors	LogP lipophilicity	Molar refractivity	No of violations
66	91694722	Trans-2-Decen-1-ol, trifluoroacetate	252	0	2	4.008599	59.52999	0
67	112657	Nonadien-1-ol	140	1	1	2.2813	44.89079	0
68	598776	Imidazo(1,2-a)pyridine,3-cyanomethyl-6-methyl-	171	0	2	1.7088	49.24599	0
69	598775	3,3'-Dipyridylamine\$N-(3-Pyridinyl)-3-pyridinamine	171	1	3	2.2202	51.7567	0
70	598364	Bicyclo[4.1.0]heptan-2-ol,1-phenyl-, endo-	188	1	1	2.4891	56.08479	0
71	592567	2-[(3,5-Dimethyl-1H-pyrazol-1-ylmethyl)-amino]-5,5-dimethyl-5,6-dihydro-4H-benzothiazole-7-one	304	1	4	2.94844	82.93719	0
72	135587489	6-Amino-2-(pyrrolidin-1-yl)-3H-pyrimidin-4-one	180	3	5	-0.6319	48.6551	0
73	75953512	(2R,3R,4ar,5S,8as)-2-Hydroxy-4a,5-dimethyl-3-(prop-1-en-2-yl)octahydronaphthalen-1(2H)-one	224	2	2	2.1905	62.83958	0
74	5375838	(3Z)-3-([(4-Methyl-5-oxo-3-(phenylsulfanyl)tetrahydro-2-furanyl]oxy)methylene)-3,3a,4,6a-tetrahydro-2H-cyclopenta[b]furan-2-one#	358	0	5	3.068299	91.42598	0
75	590981	9-t-Butyltricyclo[4.2.1.1(2,5)]decane-9,10-diol	224	2	2	2.1905	62.83958	0
76	175005	Propanoicacid,3,3'-thiobis-, dimethylester	234	0	4	1.3378	59.68499	0
Control	31703	Doxorubicin	543	7	12	-0.4641	129.8884	3

**Table 2.** SwissADME analysis of phytochemicals from *B. albus*.

S. No	Compounds	Water solubility	Gi-absorption	BBB permanent	P-gpsubstrate	CYP3A4 Inhibitor	Bioavailability
Control	Doxorubicin	-3.91 Soluble	Low	No	Yes	No	0.17
1	4-[(2-Hydroxy-phenylimino)-methyl]-5-methyl-2-phenyl-2,4-dihydro-pyrazol-3-one	-3.43 Soluble	High	Yes	No	No	0.55
2	Calcifediol	-5.82 Moderately soluble	High	No	No	No	0.55
3	2-(6-{1-ethyl-4-[4-(1H-pyrrol-2-ylcarbonyl)-2,3,3a,4,5,7a-hexahydro-1H-inden-5-yl]-1,3-butadienyl}-5-methyltetrahydro-2H-pyran-2-yl)propanoate	-6.44 Poorly soluble	High	No	Yes	Yes	0.56
4	2-[(3,5-Dimethyl-1H-pyrazol-1-ylmethyl)-amino]-5,5-dimethyl-5,6-dihydro-4H-benzothiazole-7-one	-4.94 Moderately soluble	High	No	Yes	No	0.55
5	(2R,3R,4aR,5S,8aS)-2-Hydroxy-4a,5-dimethyl-3-(prop-1-en-2-yl)octahydronaphthalen-1(2H)-one	-3.57 Soluble	High	Yes	No	No	0.55
6	(3Z)-3-((4-Methyl-5-oxo-3-(phenylsulfanyl)tetrahydro-2-furanyl)oxy)methylene)-3,3a,4,6a-tetrahydro-2H-cyclopenta[b]furan-2-one#	-4.18 Moderately soluble	High	No	No	Yes	0.56
7	9-t-Butyltricyclo[4.2.1.1(2,5)]decane-9,10-diol	-1.55 Soluble	High	Yes	No	No	0.55
8	Methyl5,7-hexadecadiynoate	-4.32 Moderately soluble	High	Yes	No	No	0.55
9	Bicyclo[4.1.0]heptan-2-ol,1-phenyl-,endo-	-3.29 Soluble	High	Yes	No	No	0.55

The ligand-binding affinity of the apoptotic proteins was screened, and phytochemicals with binding affinities greater than -5.5 kcal/mol were set as the cut-off. After screening ligand-binding affinities, the phytochemicals were subjected to molecular docking, and their binding energies were evaluated individually. Doxorubicin was used as a standard drug, and the binding affinities are -7.4 kcal/mol, and their binding energies vary as -5.96 and -2.92 for Bcl2 and BAX, respectively. The phytochemicals from *B. albus* had similar and higher binding affinities, and the same was observed for the binding energies (Tables 3 and 4).

**Table 3.** Binding affinities and binding energies of phytochemicals of *B. albus* with Bcl-2.

S. No	Compounds	Binding affinity (kcal/mol) (PyRX)	Binding energy (kcal/mol)– AutoDock
1	benzenesulfonamide,3-amino-N-methyl-N-octadecyl-	-6.3	-5.16
2	Dodecylnonylether	-5.5	-4.4
3	9-octadecenoicacid(z)-	-5.7	-0.03
4	4-[(2-Hydroxy-phenylimino)-methyl]-5-methyl-2-phenyl-2,4-dihydro-pyrazol-3-one	-7.4	-6.76
5	2,6-Dihydroxybenzaldehyde,carbamoylhydrazone	-5.8	-4.65

S. No	Compounds	Binding affinity (kcal/mol) (PyRX)	Binding energy (kcal/mol)– AutoDock
6	Calcifediol	-8.1	-6.87
7	2-(6-{1-ethyl-4-[4-(1H-pyrrol-2-ylcarbonyl)-2,3,3a,4,5,7a-hexahydro-1H-inden-5-yl]-1,3-butadienyl}-5-methyltetrahydro-2H-pyran-2-yl)propanoate	-7.8	-8.38
8	Phenol,3,5-bis(1,1-dimethylethyl)-	-5.9	-5.44
9	Pyrrolo[1,2-a]pyrazine-1,4-dione,hexahydro-	-5.5	-4.93
10	1,4-diaza-2,5-dioxobicyclo[4.3.0]nonane	-5.9	-5.05
11	Benzenepropanoicacid,3,5-bis(1,1-dimethylethyl)-4-hydroxy-,methylester	-6.2	-5.83
12	4-(3,5-Di-tert-butyl-4-hydroxyphenyl)butylacrylate	-6.4	-5.86
13	Methyl5,7-hexadecadiynoate	-5.7	-5.1
14	Methyl9,11-octadecadiynoate	-5.6	-4.61
15	Methyl10,12-octadecadiynoate	-5.7	-5.52
16	trans-2-Decen-1-ol,trifluoroacetate	-5.7	-4.35
17	Imidazo(1,2-a)pyridine,3-cyanomethyl-6-methyl-	-5.6	-5.25
18	Bicyclo[4.1.0]heptan-2-ol,1-phenyl-,endo-	-6.1	-5.64
19	2-[(3,5-Dimethyl-1H-pyrazol-1-ylmethyl)-amino]-5,5-dimethyl-5,6-dihydro-4H-benzothiazole-7-one	-6.9	-6.37
20	6-Amino-2-(pyrrolidin-1-yl)-3H-pyrimidin-4-one	-6	-5.05
21	(2R,3R,4aR,5S,8aS)-2-Hydroxy-4a,5-dimethyl-3-(prop-1-en-2-yl)octahydronaphthalen-1(2H)-one	-6.2	-6.26
22	(3Z)-3-((4-Methyl-5-oxo-3-(phenylsulfanyl)tetrahydro-2-furanyl]oxy)methylene)-3,3a,4,6a-tetrahydro-2H-cyclopenta[b]furan-2-one#	-7.7	-7.56
23	9-t-Butyltricyclo[4.2.1.1(2,5)]decane-9,10-diol	-6	-5.96
24	Doxorubicin	-7.4	-5.96

**Table 4.** Binding affinities and binding energies of phytochemicals of *B.albus* with Bax.

S. No	Compounds	Binding affinity (kcal/mol) (PyRX)	Binding energy (kcal/mol)–AutoDock
1	benzenesulfonamide,3-amino-N-methyl-N-octadecyl-	-6.3	-2.06
2	Dodecylnonylether	-5.5	-3.14
3	9-octadecenoicacid(z)-	-5.7	2.65
4	4-[(2-Hydroxy-phenylimino)-methyl]-5-methyl-2-phenyl-2,4-dihydro-pyrazol-3-one	-7.4	-7.63
5	2,6-Dihydroxybenzaldehyde,carbamoylhydrazone	-5.8	-5.63
6	Calcifediol	-8.1	-8.28
7	2-(6-{1-ethyl-4-[4-(1H-pyrrol-2-ylcarbonyl)-2,3,3a,4,5,7a-hexahydro-1H-inden-5-yl]-1,3-butadienyl}-5-methyltetrahydro-2H-pyran-2-yl)propanoate	-7.8	-5.42
8	Phenol,3,5-bis(1,1-dimethylethyl)-	-5.9	-5.9
9	Phenol,2,6-bis(1,1-dimethylethyl)-	-5.6	-5.26
10	Pyrrolo[1,2-a]pyrazine-1,4-dione,hexahydro-	-5.5	-4.78
11	1,4-diaza-2,5-dioxobicyclo[4.3.0]nonane	-5.9	-5.33
12	Benzenepropanoicacid,3,5-bis(1,1-dimethylethyl)-4-hydroxy-,methylester	-6.2	-5.13
13	4-(3,5-Di-tert-butyl-4-hydroxyphenyl)butylacrylate	-6.4	-5.02
14	Methyl5,7-hexadecadiynoate	-5.7	-7.24
15	Methyl9,11-octadecadiynoate	-5.6	-5.4
16	Methyl10,12-octadecadiynoate	-5.7	-5.48
17	:trans-2-Decen-1-ol,trifluoroacetate	-5.7	-5.45
18	Imidazo(1,2-a)pyridine,3-cyanomethyl-6-methyl-	-5.6	-5.86
19	Bicyclo[4.1.0]heptan-2-ol,1-phenyl-,endo-	-6.1	-6.6
20	2-[(3,5-Dimethyl-1H-pyrazol-1-ylmethyl)-amino]-5,5-dimethyl-5,6-dihydro-4H-benzothiazole-7-one	-6.9	-6.91

S. No	Compounds	Binding affinity (kcal/mol) (PyRX)	Binding energy (kcal/mol)–AutoDock
21	6-Amino-2-(pyrrolidin-1-yl)-3H-pyrimidin-4-one	-6	-5.3
22	(2R,3R,4aR,5S,8aS)-2-Hydroxy-4a,5-dimethyl-3-(prop-1-en-2-yl)octahydronaphthalen-1(2H)-one	-6.2	-6.74
23	(3Z)-3-((4-Methyl-5-oxo-3-(phenylsulfanyl)tetrahydro-2-furanyl)oxy)methylene)-3,3a,4,6a-tetrahydro-2H-cyclopenta[b]furan-2-one#	-7.7	-6.37
24	9-t-Butyltricyclo[4.2.1.1(2,5)]decane-9,10-diol	-6	-6.18
25	Doxorubicin	-7.4	-2.92

For Bcl2, 2-(6-{1-ethyl-4-[4-(1H-pyrrol-2-ylcarbonyl)-2,3,3a,4,5,7a-hexahydro-1H-inden-5-yl]-1,3-butadienyl}-5-methyltetrahydro-2H-pyran-2-yl) propanoate showed a higher binding affinity of -7.8 kcal/mol, whereas its binding energy was higher than the binding affinity, which was found as -8.38 kcal/mol. Similarly, (3Z)-3-((4-Methyl-5-oxo-3-(phenyl sulfonyl)tetrahydro-2-furanyl)oxy)methylene)-3,3a,4,6a-tetrahydro-2H-cyclopenta[b]furan-2-one# had a binding affinity of -7.7kcal/mol, and its binding energy is similar to the binding affinity, and it was found as -7.56 kcal/mol. For BAX, Calcifediol showed a higher binding affinity of -8.1 kcal/mol, and its binding energy with BAX was higher than the binding affinity of -8.28 kcal/mol. Similarly, phytochemicals like 4-[(2-Hydroxy-phenylamino)-methyl]-5-methyl-2-phenyl-2,4-dihydro-pyrazol-3-one, Bicyclo[4.1.0]heptan-2-ol,1-phenyl-, endo-,2-[(3,5-Dimethyl-1H-pyrazol-1-ylmethyl)-amino]-5,5-dimethyl-5,6-dihydro-4H-benzothiazol-7-one,(2R,3R,4aR,5S,8aS)-2-Hydroxy-4a,5-dimethyl-3-(prop-1-en-2-yl)octahydronaphthalen-1(2H)-one,9-t-Butyltricyclo[4.2.1.1(2,5)]decane-9,10-diol had similar binding energies as that of their binding affinity (Table- BAX). The phytochemicals from *B. albus* interacted with Bcl-2 and Bax, forming conventional hydrogen bonds. Doxorubicin with Bcl2 formed 4 conventional hydrogen bonds with GLN 13, LYS 17, HIS 20, and GLU 42, whereas BAX and doxorubicin formed one conventional hydrogen bond with GLN 146. with Calcifediol which was able to form one hydrogen bond at LEU 120 (Figure 3).

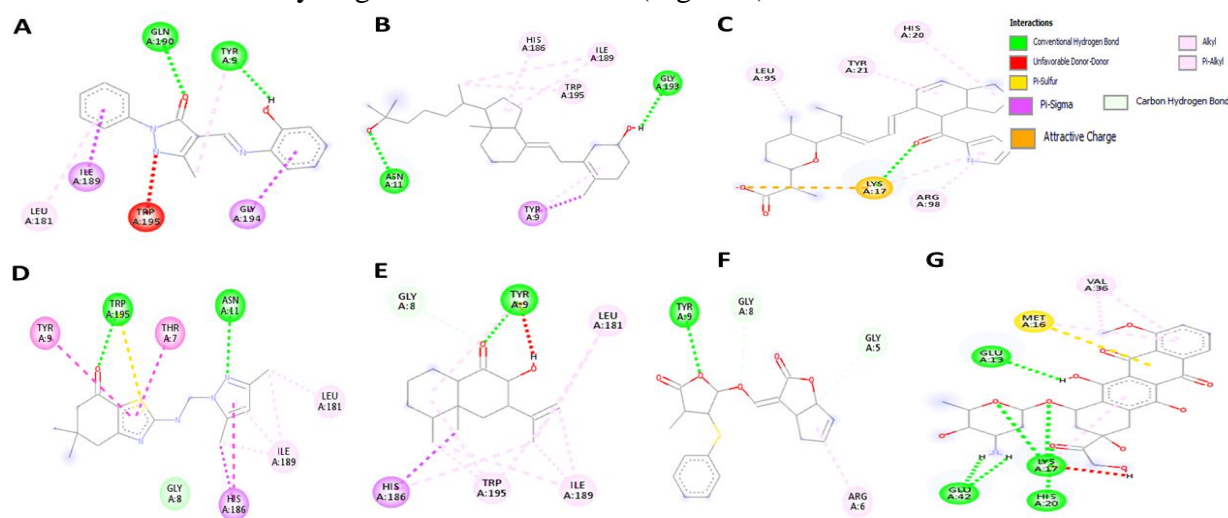


**Figure2.** Interactions of phytochemicals with Bcl2 (A) 4-[(2-Hydroxy-phenylamino)-methyl]-5-methyl-2-phenyl-2,4-dihydro-pyrazol-3-one; (B) Calcifediol; (C) 2-(6-{1-ethyl-4-[4-(1H-pyrrol-2-ylcarbonyl)-2,3,3a,4,5,7a-hexahydro-1H-inden-5-yl]-1,3-butadienyl}-5-methyltetrahydro-2H-pyran-2-yl)propanoate; (D) 2-[(3,5-Dimethyl-1H-pyrazol-1-ylmethyl)-amino]-5,5-dimethyl-5,6-dihydro-4H-benzothiazol-7-one; (E) (2R,3R,4aR,5S,8aS)-2-Hydroxy-4a,5-dimethyl-3-(prop-1-en-2-yl)octahydronaphthalen-1(2H)-one; (F) (3Z)-3-((4-Methyl-5-oxo-3-(phenylsulfanyl)tetrahydro-2-furanyl)oxy)methylene)-3,3a,4,6a-tetrahydro-2H-cyclopenta[b]furan-2-one#; (G) Doxorubicin.

The highest binding energy for Bcl2 is with 2-(6-{1-ethyl-4-[4-(1H-pyrrol-2-ylcarbonyl)-2,3,3a,4,5,7a-hexahydro-1H-inden-5-yl]-1,3-butadienyl}-5-methyltetrahydro-2H-pyran-2-yl)propanoate, which was able to form one hydrogen bond at LYS 17 (Figure 2), and for BAX, the highest binding energy was observed

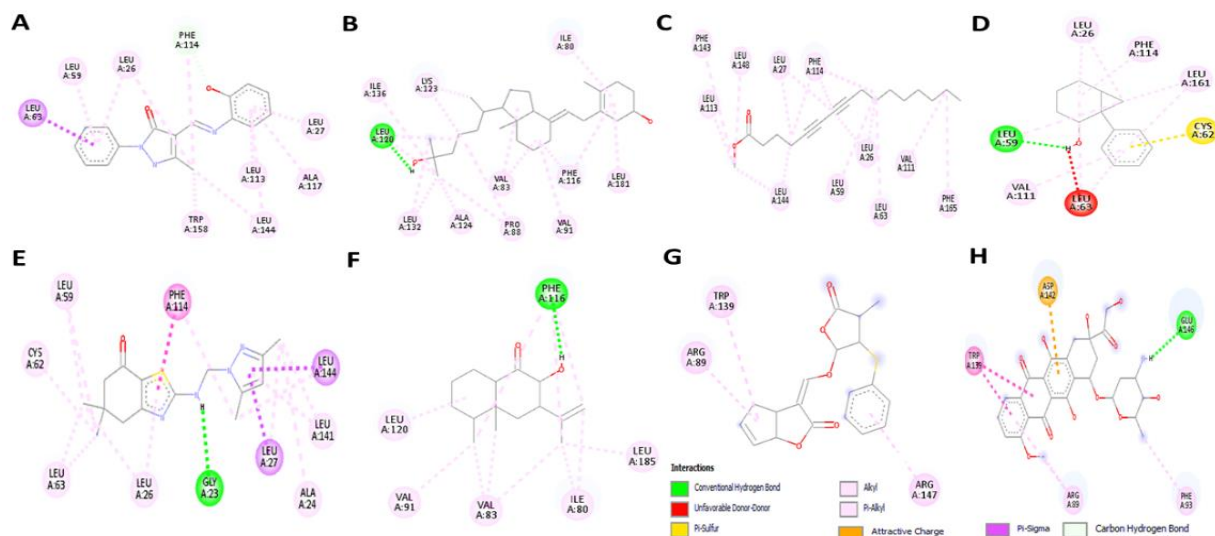


**Figure 3.** Interactions of phytochemicals with Bcl2 (A) 4-[(2-Hydroxy-phenylimino)-methyl]-5-methyl-2-pyridyl-2,4-dihydro-pyrazol-3-one; (B) Calcifediol; (C) Methyl5,7-hexadecadienoate; (D) Bicyclo[4.1.0]heptan-2-ol,1-phenyl-endo; (E) 2-[(3,5-Dimethyl-1H-pyrazol-1-ylmethyl)-amino]-5,5-dimethyl-5,6-dihydro-4H-benzothiazol-7-one; (F) (2R,3R,4aR,5S,8aS)-2-Hydroxy-4a,5-dimethyl-3-(prop-1-en-2-yl)octahydronaphthalen-1(2H)-one; (G) (3Z)-3-([(4-Methyl-5-oxo-3-(phenylsulfanyl)tetrahydro-2-furanyl)oxy)methylene]-3,3a,4,6a-tetrahydro-2H-cyclopenta[b]furan-2-one#; (H) Doxorubicin.

SwissADME analysis of *B. albus* phytochemicals revealed that, on average, the compounds are soluble except 2-(6-{1-ethyl-4-[4-(1H-pyrrol-2-ylcarbonyl)-2,3,3a,4,5,7a-hexahydro-1H-inden-5-yl]-1,3-butadienyl}-5-methyltetrahydro-2H-pyran-2-yl) propanoate, which is poorly soluble. All the phytochemicals have a high  $G_i$ -absorption rate and are highly bioavailable except the standard drug. Overexpression of P-glycoproteins in cancer cells is a significant therapeutic barrier that results in drug efflux and renders chemotherapy largely ineffective. Therefore, the ideal ligands for cancer therapy are those that are not P-gp substrates [23]. Hence doxorubicin, 2-(6-{1-ethyl-4-[4-(1H-pyrrol-2-ylcarbonyl)-2,3,3a,4,5,7a-hexahydro-1H-inden-5-yl]-1,3-butadienyl}-5-methyltetrahydro-2H-pyran-2-yl)propanoate and 2-[(3,5-Dimethyl-1H-pyrazol-1-ylmethyl)-amino]-5,5-dimethyl-5,6-dihydro-4H-benzothiazol-7-one cannot be considered. Most phytochemicals are not inhibitors of CYP3A4 and are members of the cytochrome P450 enzyme family, which is crucial in drug metabolism. When a drug interacts with cytochrome P450 isoenzymes, it may either cause rapid metabolism if it is a CYP substrate that induces, or cause accumulation if it is an inhibitor [23].

The ligand binding affinity of doxorubicin with Bcl-2 and Bax was -7.4 kcal/mol, and their binding energies varied between -5.96 and -2.92 for Bcl-2 and BAX, respectively. The Bcl2 was able to interact more with 2-(6-{1-ethyl-4-[4-(1H-pyrrol-2-ylcarbonyl)-2,3,3a,4,5,7a-hexahydro-1H-inden-5-yl]-1,3-butadienyl}-5-methyltetrahydro-2H-pyran-2-yl)propanoate, showing a higher binding affinity of -7.8 kcal/mol. In contrast, its binding energy was higher than its binding affinity, which was -8.38 kcal/mol. Bax interacted strongly with Calcifediol, showing a higher binding affinity of -8.1kcal/mol, and its binding energy with Bax was -8.28 kcal/mol. The above results suggest that the binding affinities and binding energies are higher

for the phytochemicals of *B. albus* than for the standard drug doxorubicin, and all these compounds were able to form conventional hydrogen bonds. Further, it is observed that the ratio of binding of phytochemicals varies with Bcl-2 (anti-apoptotic protein) and Bax (pro-apoptotic protein). Hence, it can be said that the ratio of molecules binding to Bax can influence the death of cancerous cells. Doxorubicin is also known as the red devil and is widely used as a chemotherapeutic drug. It is effective against various types of cancer, including breast cancer, lung cancer, sarcomas, and leukemias. The mechanism of action of doxorubicin is to inhibit topoisomerase 2, which helps control the growth of cancerous cells, induces apoptosis, disrupts membrane integrity, and generates ROS. The one drawback is that they target both healthy and cancerous cells, leading to side effects [24]. 2-(6-{1-ethyl-4-[4-(1H-pyrrol-2-ylcarbonyl)-2,3,3a,4,5,7a-hexahydro-1H-inden-5-yl]-1,3-butadienyl}-5-methyltetrahydro-2H-pyran-2-yl)propanoate contains a pyran group, and this group of molecules is known to have various biological properties. Naturally derived pyran group molecules are polyphenolic compounds known to exhibit antibacterial, anti-inflammatory, and anticancer activities. One such pyran molecule is curcumin, which contains a pyran ring and is known for the above-mentioned properties. Curcumin is well-known for its anticancer properties and has established mechanisms of action, including i) induction of apoptosis, ii) modulation of signaling pathways, iii) interference in the inflammation mechanism, and iv) controlling tumor growth and metastasis [25]. To corroborate our results, 2-(6-{1-ethyl-4-[4-(1H-pyrrol-2-ylcarbonyl)-2,3,3a,4,5,7a-hexahydro-1H-inden-5-yl]-1,3-butadienyl}-5-methyltetrahydro-2H-pyran-2-yl)propanoate can induce apoptosis and regulate the expression of Bcl-2 and Bax, disrupt the mitochondrial functions, and activate caspases. Calcifediol, also known as 1,25-dihydroxy vitamin D<sub>3</sub>, is a precursor molecule for the active form of Vitamin D. Calcifediol and their analogs and derivatives are known to i) regulate the cell growth and differentiation process in both normal and cancerous cells by interacting with Vitamin D receptors which are usually present in both the cells and these derivatives can modulate the expression of genes involved in cell proliferation, differentiation and apoptosis, ii) Calcifediol active form calcitriol is known induce apoptosis in cancer cells by activating Vitamin D receptors which induces expression of pro-apoptotic genes and down-regulate anti-apoptotic factors, iii) Calcifediol also modulates the balance of cell cycle proteins including cyclins and cyclin-dependent kinases which affect the growth and proliferation of cancerous cells [26]. Calcifediol strongly binds to Bax and can induce apoptosis to corroborate our results.

### 3.3. Characterization of AgNPs.

The biosynthesis of silver nanoparticles was optimized by considering parameters such as nanoparticle yield, stability, synthesis duration, and color change from pale yellow to reddish brown, confirming the synthesis. The characterizations of the synthesized AgNPs also confirmed the successful biosynthesis of silver nanoparticles. The primary characterization was performed using UV-visible spectroscopy; a surface plasmon resonance (SPR) peak at 430 nm was observed, confirming the silver nanoparticle synthesis (Figure 4A). FT-IR spectroscopy revealed the functional groups and the bond interactions present in the AgNPs. The peak at 3248.5 cm<sup>-1</sup> confirmed the presence of alcohols and phenols; the peak at 2938.98 cm<sup>-1</sup> revealed the presence of alkanes; the peak at 1990.18 cm<sup>-1</sup> and 1634.38 cm<sup>-1</sup> confirmed the presence of alkenes; the peak at 1404.89 cm<sup>-1</sup>, 1116.58 cm<sup>-1</sup>, and 613.252 cm<sup>-1</sup> confirmed the presence of aldehydes and ketones, amines and alkynes, respectively (Figure 4B). The morphological analysis of the AgNPs, as revealed by FESEM, showed that the nanoparticles were cubic in

shape (Figure 4E). Through DLS analysis, the average hydrodynamic size of the nanoparticles was 50.6 nm, and the PDI (polydispersity index) was 0.574, indicating polydispersity (Figure 4C). A PDI value of 0.1 means the nanoparticles are highly monodispersed, and a PDI value of 0.9 means the nanoparticles are highly polydispersed. The EDX analysis also confirmed the synthesis of silver nanoparticles, as evidenced by the Ag peak at 3 keV (Figure 4F).

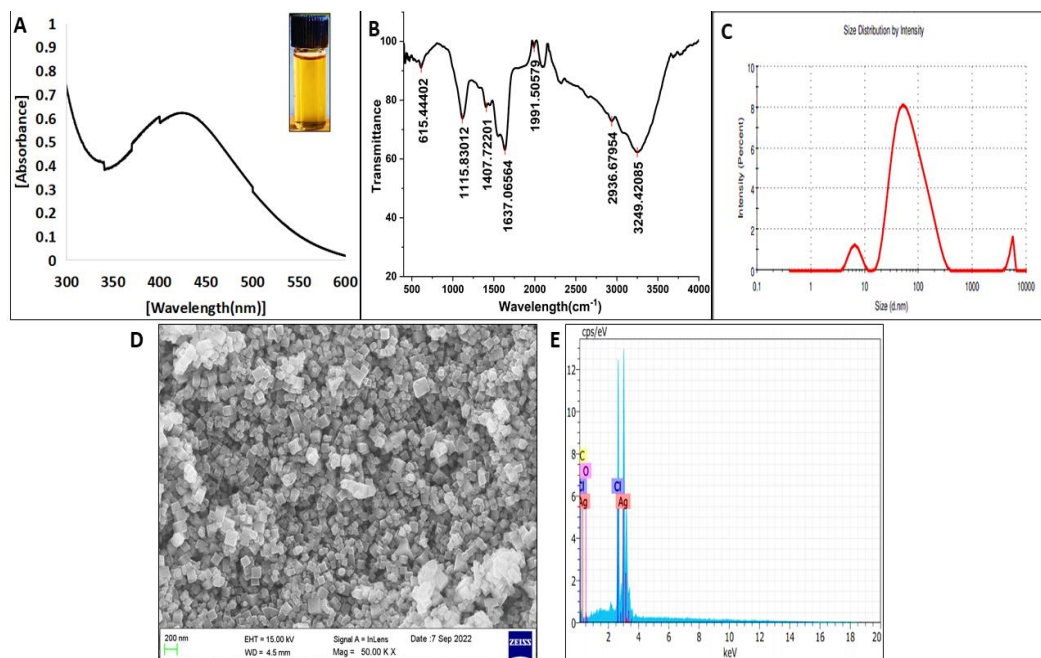


**Figure 4.** (A) UV-Visible spectrum of AgNPs; (B) FT-IR of AgNPs; (C) DLS of AgNPs; (D) FESEM of AgNPs; (E) EDAX of AgNPs.

The *B. albus* crude extract was used to synthesize silver nanoparticles, and a color change from pale yellow to reddish brown was observed. The color change is due to the reduction of silver ions to silver, and these silver nanoparticles are stabilized by the capping agents, which help prevent particle aggregation. The reduction and capping of silver nanoparticles occur due to phytochemicals in *B. albus* extract. The synthesized AgNPs were characterized by UV-visible spectroscopy, with a surface plasmon resonance peak at 430 nm. FT-IR was performed to analyze the functional groups present in AgNPs, including aldehydes and ketones, amines and alkynes, alcohols, and phenols. The DLS was employed to analyze the hydrodynamic size and polydispersity of AgNPs, revealing that they are polydispersed, with a size of 50.6 nm and confined to the nanoscale. The FESEM was performed to determine the size and shape of the AgNPs, and reports reveal that the AgNPs are cubical in shape. EDAX was performed to analyze the elemental composition of AgNPs; they contain Ag, Cl, O, and C, and these elements may have assisted in the reduction and capping of AgNPs during synthesis. Previous reports have synthesized silver nanoparticles from the endophytic bacterium *Cronobacter sakazakii*, showing similar results [27].

#### 3.4. AgNPs induce cytotoxicity in MDA-MB-231 cell lines.

Cell viability results revealed that the AgNPs induced cytotoxicity in MDA-MB-231 at the higher concentration of 20  $\mu\text{g/ml}$  after 24 hours. In control, the percentage of viable cells is 100%, and the AgNPs-treated MDA-MB-231 cells at varied concentrations are 92%, 89%, 76%, and 48% at 2.5, 5, 10, and 20  $\mu\text{g/ml}$ , respectively (Figure 5B). The morphological alterations of MDA-MB-231 are shown in Figure 5A, and these changes are dose-dependent

in Figure 5A. Triple negative breast cancer (TNBC) is a subtype of breast cancer, and it is characterized by the absence of human epidermal growth factor receptor (HER-2), progesterone receptor (PR), and estrogen receptor (ER). TNBCs are aggressive and are difficult to treat [28].

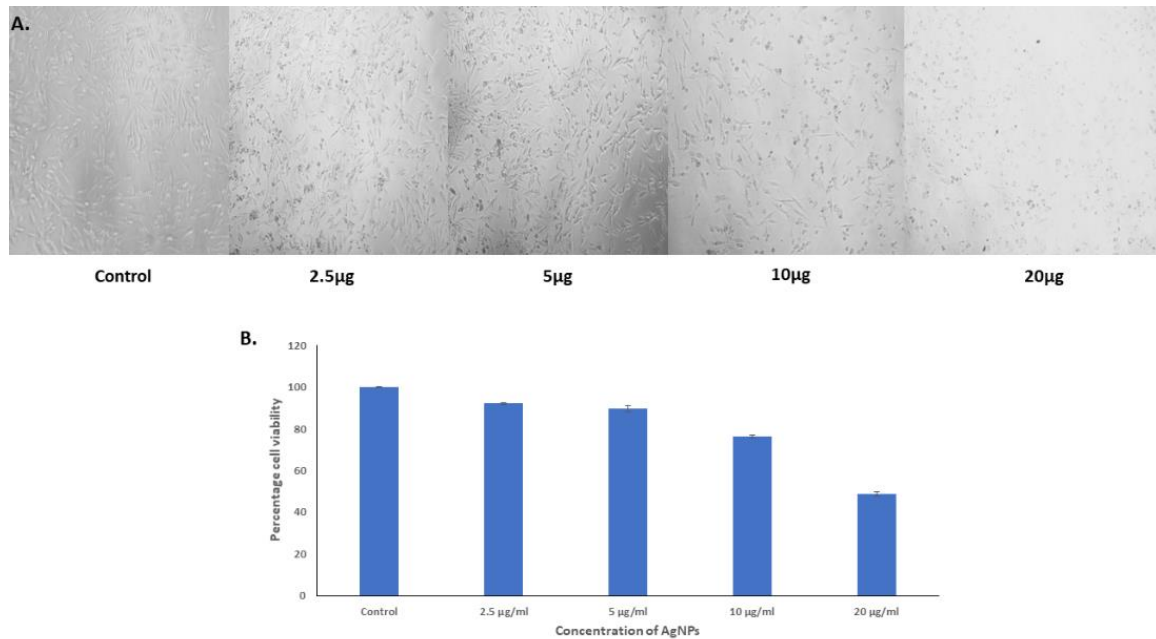


**Figure 5.** (A) Morphological alterations in MDM-MB-231 treated cells; (B) Percentage of cell viability in AgNPs in MDM-MB-231 treated cells.

Hence, nanotechnology can be employed to treat TNBC, as nanoparticles can easily penetrate cells and induce cytotoxicity. Cell viability assay was performed in triple-negative breast cancer cell lines (MDA-MB-231), and the AgNPs from *B. albus* were able to induce cytotoxicity and kill fifty percent of the population of cells at 20 µg/ml. Previous studies reported that silver nanoparticles isolated from endophytic bacteria of the ornamental plant *Pennisetum setaceum* induced nearly 50% cell death at 50 µg/ml. Also, these silver nanoparticles induced apoptosis by upregulating Bax and downregulating Bcl-2 in MCF-7 cells by Western blot analysis [27]. Similarly, AgNPs from *Penicillium oxalicum* showed an IC<sub>50</sub> value of 20 µg/ml in MDA-MB-231 treated cells [29]. The mechanism of action of silver nanoparticles includes i) generation of ROS– increased levels of ROS induce DNA damage and lipid peroxidation and disrupt the cellular mechanisms, ii) induction of apoptosis, iii) Interference with cell survival and cell signaling proteins, and iv) silver nanoparticles modulate the immune response and induce Tc (immune cell- mediated cytotoxic) responses [30]. Overall, our results show that the crude extract of *B. albus* binds pro-apoptotic proteins and downregulates anti-apoptotic proteins, and that silver nanoparticles, in synergy with phytocompounds from *B. albus*, can induce apoptosis via the intrinsic pathway.

#### 4. Conclusions

The absence of hormonal receptors characterizes triple-negative breast cancer (TNBC) and is poorly diagnosed. TNBC is highly aggressive and difficult to treat. Hence, in this study, endophytic bacteria were isolated from seaweed, and they were identified as *B. albus*. *In silico* screening was performed for the phytocompounds present in *B. albus*, and all compounds demonstrated drug-like properties and bound to apoptotic proteins. Then, eco-friendly, cost-

effective silver nanoparticles were synthesized from the *B. albus* extract and characterized by various methods, revealing that the nanoparticles are cubical in shape and polydispersed. The AgNPs were able to induce cytotoxicity in MDA-MB-231-treated cells in a dose-dependent manner. The AgNPs produced from endophytic bacteria isolated from plants can be used to create nanoformulations that can be used as a therapeutic agent for the treatment of cancer, and further *in vivo* studies are warranted.

### Author Contributions

Conceptualization, H.S.; methodology, H.S., S.A.M., M.J.N.A.; software, H.S.; validation, H.S.; formal analysis, H.S., S.A.M., M.J.N.A.; investigation, H.S., S.A.M., M.J.N.A.; resources, H.S.; writing—original draft preparation, H.S., S.A.M., M.J.N.A.; writing—review and editing, H.S.; visualization, H.S., S.A.M., M.J.N.A.; supervision, H.S.; project administration, H.S. All authors have read and agreed to the published version of the manuscript.

### Institutional Review Board Statement

Not applicable.

### Informed Consent Statement

Not applicable.

### Data Availability Statement

Data supporting the findings of this study are available upon reasonable request from the corresponding author.

### Funding

This research did not receive any external funding.

### Acknowledgments

The authors are thankful to the School of Life Sciences, B. S. Abdur Rahman Crescent Institute of Science and Technology, for providing the research facilities.

### Conflicts of Interest

The authors declare no conflict of interest.

### References

1. Ataollahi, M.R.; Sharifi, J.; Paknahad, M.R.; Paknahad, A. Breast cancer and associated factors: a review. *J. Med. Life* **2015**, *8*, 6–11.
2. Gucalp, A.; Traina, T.A.; Eisner, J.R.; Parker, J.S.; Selitsky, S.R.; Park, B.H.; Elias, A.D.; Baskin-Bey, E.S.; Cardoso, F. Male breast cancer: a disease distinct from female breast cancer. *Breast Cancer Res. Treat.* **2019**, *173*, 37–48, <https://doi.org/10.1007/s10549-018-4921-9>.
3. Łukasiewicz, S.; Czaczelewski, M.; Forma, A.; Baj, J.; Sitarz, R.; Stanisławek, A. Breast Cancer—Epidemiology, Risk Factors, Classification, Prognostic Markers, and Current Treatment Strategies—An Updated Review. *Cancers* **2021**, *13*, 4287, <https://doi.org/10.3390/cancers13174287>.

4. Koo, M.M.; von Wagner, C.; Abel, G.A.; McPhail, S.; Rubin, G.P.; Lyratzopoulos, G. Typical and atypical presenting symptoms of breast cancer and their associations with diagnostic intervals: Evidence from a national audit of cancer diagnosis. *Cancer Epidemiol.* **2017**, *48*, 140-146, <https://doi.org/10.1016/j.canep.2017.04.010>.
5. Burguin, A.; Diorio, C.; Durocher, F. Breast Cancer Treatments: Updates and New Challenges. *J. Pers. Med.* **2021**, *11*, 808, <https://doi.org/10.3390/jpm11080808>.
6. Cao, J.; Zhang, M.; Wang, B.; Zhang, L.; Zhou, F.; Fang, M. Chemoresistance and Metastasis in Breast Cancer Molecular Mechanisms and Novel Clinical Strategies. *Front. Oncol.* **2021**, *11*, 658552, <https://doi.org/10.3389/fonc.2021.658552>.
7. Tang, X.; Loc, W.S.; Dong, C.; Matters, G.L.; Butler, P.J.; Kester, M.; Meyers, C.; Jiang, Y.; Adair, J.H. The Use of Nanoparticulates to Treat Breast Cancer. *Nanomedicine* **2017**, *12*, 2367-2388, <https://doi.org/10.2217/nmm-2017-0202>.
8. Yan, X.; Zhou, M.; Yu, S.; Jin, Z.; Zhao, K. An overview of biodegradable nanomaterials and applications in vaccines. *Vaccine* **2020**, *38*, 1096-1104, <https://doi.org/10.1016/j.vaccine.2019.11.031>.
9. Ratan, Z.A.; Mashrur, F.R.; Chhoan, A.P.; Shahriar, S.M.; Haidere, M.F.; Runa, N.J.; Kim, S.; Kweon, D.-H.; Hosseinzadeh, H.; Cho, J.Y. Silver Nanoparticles as Potential Antiviral Agents. *Pharmaceutics* **2021**, *13*, 2034, <https://doi.org/10.3390/pharmaceutics13122034>.
10. Bhattacharya, D.; Gupta, R.K. Nanotechnology and Potential of Microorganisms. *Crit. Rev. Biotechnol.* **2005**, *25*, 199-204, <https://doi.org/10.1080/07388550500361994>.
11. Yang, Z.; Chang, Z.; Sun, L.; Yu, J.; Huang, B. Physiological and Metabolic Effects of 5-Aminolevulinic Acid for Mitigating Salinity Stress in Creeping Bentgrass. *PLoS One* **2014**, *9*, e116283, <https://doi.org/10.1371/journal.pone.0116283>.
12. Singh, M.; Kumar, A.; Singh, R.; Pandey, K.D. Endophytic bacteria: a new source of bioactive compounds. *3 Biotech.* **2017**, *7*, 315, <https://doi.org/10.1007/s13205-017-0942-z>.
13. Carpena, M.; Garcia-Perez, P.; Garcia-Oliveira, P.; Chamorro, F.; Otero, P.; Lourenço-Lopes, C.; Cao, H.; Simal-Gandara, J.; Prieto, M.A. Biological properties and potential of compounds extracted from red seaweeds. *Phytochem. Rev.* **2023**, *22*, 1509-1540, <https://doi.org/10.1007/s11101-022-09826-z>.
14. Teixeira, T.R.; Santos, G.S.d.; Armstrong, L.; Colepicolo, P.; Deboni, H.M. Antitumor Potential of Seaweed Derived-Endophytic Fungi. *Antibiotics* **2019**, *8*, 205, <https://doi.org/10.3390/antibiotics8040205>.
15. Singh, D.; Rathod, V.; Ninganagouda, S.; Hiremath, J.; Singh, A.K.; Mathew, J. Optimization and Characterization of Silver Nanoparticle by Endophytic Fungi *Penicillium* sp. Isolated from *Curcuma longa* (Turmeric) and Application Studies against MDR *E. coli* and *S. aureus*. *Bioinorg. Chem. Appl.* **2014**, *2014*, 408021, <https://doi.org/10.1155/2014/408021>.
16. Janda, J.M.; Abbott, S.L. 16S rRNA Gene Sequencing for Bacterial Identification in the Diagnostic Laboratory: Pluses, Perils, and Pitfalls. *J. Clin. Microbiol.* **2007**, *45*, 2761-2764, <https://doi.org/10.1128/JCM.01228-07>.
17. Edet, M.L.; Hemalatha, S. Identification of natural CTXM-15 inhibitors from aqueous extract of endophytic bacteria *Cronobacter sakazaki*. *Braz. J. Microbiol.* **2023**, *54*, 827-839, <https://doi.org/10.1007/s42770-023-00945-z>.
18. Lipinski, C.A. Lead-and drug-like compounds: the rule-of-five revolution. *Drug Discov. Today: Technol.* **2004**, *1*, 337-341, <https://doi.org/10.1016/j.ddtec.2004.11.007>.
19. Daina, A.; Michielin, O.; Zoete, V. SwissADME: a free web tool to evaluate pharmacokinetics, drug-likeness and medicinal chemistry friendliness of small molecules. *Sci. Rep.* **2017**, *7*, 42717, <https://doi.org/10.1038/srep42717>.
20. Ravindranath, K.J.; Christian, S.D.; Srinivasan, H. Screening of Anti-carcinogenic Properties of Phytocompounds from *Allium ascalonicum* for Treating Breast Cancer Through In Silico and In Vitro Approaches. *Appl. Biochem. Biotechnol.* **2023**, *195*, 1136-1157, <https://doi.org/10.1007/s12010-022-04202-1>.
21. Love, E.M.; Hemalatha, S. Toxicity Evaluation, Plant Growth Promotion, and Anti-fungal Activity of Endophytic Bacteria-Mediated Silver Nanoparticles. *Appl. Biochem. Biotechnol.* **2023**, *195*, 6309-6320, <https://doi.org/10.1007/s12010-023-04383-3>.
22. Gouda, S.; Das, G.; Sen, S.K.; Shin, H-S.; Patra, J.K. Endophytes: A Treasure House of Bioactive Compounds of Medicinal Importance. *Front. Microbiol.* **2016**, *7*, 1538. doi: 10.3389/fmicb.2016.01538.

23. Mendie, L.E.; Hemalatha, S. Molecular Docking of Phytochemicals Targeting GFRs as Therapeutic Sites for Cancer: an In Silico Study. *Appl. Biochem. Biotechnol.* **2022**, *194*, 215-231, <https://doi.org/10.1007/s12010-021-03791-7>.
24. Thorn, C.F.; Oshiro, C.; Marsh, S.; Hernandez-Boussard, T.; McLeod, H.; Klein, T.E.; Altman, R.B. Doxorubicin pathways: pharmacodynamics and adverse effects. *Pharmacogenetics Genom.* **2011**, *21*, 440-446, <https://doi.org/10.1097/FPC.0b013e328333ffb56>.
25. Khor, P.Y.; Mohd Aluwi, M.F.F.; Rullah, K.; Lam, K.W. Insights on the synthesis of asymmetric curcumin derivatives and their biological activities. *Eur. J. Med. Chem.* **2019**, *183*, 111704, <https://doi.org/10.1016/j.ejmech.2019.111704>.
26. Donati, S.; Palmi, G.; Aurilia, C.; Falsetti, I.; Miglietta, F.; Iantomasi, T.; Brandi, M.L. Rapid Nontranscriptional Effects of Calcifediol and Calcitriol. *Nutrients* **2022**, *14*, 1291, <https://doi.org/10.3390/nu14061291>.
27. Shariq Ahmed, M.; Soundhararajan, R.; Akther, T.; Kashif, M.; Khan, J.; Waseem, M.; Srinivasan, H. Biogenic AgNPs synthesized via endophytic bacteria and its biological applications. *Environ. Sci. Pollut. Res.* **2019**, *26*, 26939-26946, <https://doi.org/10.1007/s11356-019-05869-6>.
28. Stevens, K.N.; Vachon, C.M.; Couch, F.J. Genetic Susceptibility to Triple-Negative Breast Cancer. *Cancer Res.* **2013**, *73*, 2025-2030, <https://doi.org/10.1158/0008-5472.CAN-12-1699>.
29. Gupta, P.; Rai, N.; Verma, A.; Saikia, D.; Singh, S.P.; Kumar, R.; Singh, S.K.; Kumar, D.; Gautam, V. Green-Based Approach to Synthesize Silver Nanoparticles Using the Fungal Endophyte *Penicillium oxalicum* and Their Antimicrobial, Antioxidant, and *In Vitro* Anticancer Potential. *ACS Omega* **2022**, *7*, 46653–46673, <https://doi.org/10.1021/acsomega.2c05605>.
30. Mao, B.-H.; Chen, Z.-Y.; Wang, Y.-J.; Yan, S.-J. Silver nanoparticles have lethal and sublethal adverse effects on development and longevity by inducing ROS-mediated stress responses. *Sci. Rep.* **2018**, *8*, 2445, <https://doi.org/10.1038/s41598-018-20728-z>.

## Publisher's Note & Disclaimer

The statements, opinions, and data presented in this publication are solely those of the individual author(s) and contributor(s) and do not necessarily reflect the views of the publisher and/or the editor(s). The publisher and/or the editor(s) disclaim any responsibility for the accuracy, completeness, or reliability of the content. Neither the publisher nor the editor(s) assume any legal liability for any errors, omissions, or consequences arising from the use of the information presented in this publication. Furthermore, the publisher and/or the editor(s) disclaim any liability for any injury, damage, or loss to persons or property that may result from the use of any ideas, methods, instructions, or products mentioned in the content. Readers are encouraged to independently verify any information before relying on it, and the publisher assumes no responsibility for any consequences arising from the use of materials contained in this publication.